Int. J. Electrochem. Sci., 11 **(2016)** 3285 - 3295

International Journal of
ELECTROCHEMICAL
SCIENCE
www.electrochemsci.org

The Influence of Potential Scanning Rate on the Electrocatalytic Activity of Pyrolysis-treated PdO/Graphene for Ethanol Oxidation Reaction (EOR)

Yuying Chen[1], *Min Cui*[2], *Sen Li*[3], *Jing Zhao*[1], *Yan Zhang*[1], *Binjuan Wei*[1], *Keqiang Ding*[1,3*]

[1]College of Chemistry and Materials Science, Hebei Normal University, Shijiazhuang 050024, P.R. China
[2] School of Sciences, Hebei University of Science and Technology, Shijiazhuang 050018, P.R. China
[3] Fengfan Co., Ltd, Baoding, Hebei 071057, P.R. China
[*]E-mail: dkeqiang@263.net

Received: 18 February 2016 / *Accepted:* 10 March 2016 / *Published:* 1 April 2016

For the first time, the influence of potential scanning rate on the electrocatalytic activity of pyrolysis-treated PdO/Graphene (denoted as PdO/G) was investigated in this work. First, a suspension solution that contained PdO and graphene was pyrolyzed under certain conditions, and then the products were anchored on a glassy carbon (GC) electrode, leading to the formation of pyrolysis-treated PdO/G coated GC electrode. Lastly, the resultant electrodes were potentially scanned using cyclic voltammetry (CV) technique for 50 cycles at various scanning rates in a potential range, yielding four kinds of CV-treated PdO/G electrodes. In this work, the electrodes obtained at the scan rate of 5, 10, 50, 90 mV s^{-1} were, respectively, denoted as catalyst **a**, **b**, **c** and **d**. The morphologies of the samples were mainly characterized via scanning electron microscope (SEM) and transmission electron microscopy (TEM). The electrocatalytic activities of the as-prepared catalysts for ethanol oxidation reaction (EOR) were principally studied by using cyclic voltammetry (CV) and chronoamperometry (CA). The electrochemical results strongly indicated that the catalyst of PdO/G treated by 10 mV s^{-1} exhibited the best electrocatalytic performance among all the prepared catalysts. The relatively smaller particle size and higher content of Pd were thought as the major reasons for the excellent electrocatalytic activity of catalyst **b** towards EOR when compared to other catalysts.

Keywords: PdO, graphene, pyrolysis, scanning rate, ethanol oxidation reaction, electrocatalysis

1. INTRODUCTION

Of late, direct ethanol fuel cells (DEFCs) have been thought as the promising energy converters, which can directly change the chemical energy stored in ethanol into electricity, for various

doi: 10.20964/110474

kinds of portable applications [1]. The advantages of using DEFCs could be summarized as follows [2]: (1) The energy density of ethanol based fuel cells was much larger than that of methanol (8 kWh kg^{-1} vs. 6.1 kWh kg^{-1}). (2) Ethanol could be prepared from large-scale production of biomass by the process of fermentation. (3)The storage and transportation of ethanol is easier when compared to the gas (like hydrogen) fuel. (4) Compared to methanol, the toxicity of ethanol is lower. Except for above merits, the main drawbacks of DEFCs, i.e., the higher cost of Pt catalysts employed and the slow kinetics of electro-oxidation of ethanol, were also claimed recently, which greatly hindered the further commercialization of DEFCs. Thus, the development of electrocatalysts for ethanol oxidation reaction (EOR) has turned into a major challenge for electrochemical researcher [3]. Fortunately, very recently, palladium (Pd), which is cheaper and at least 50 times more abundant than Pt [4], has been demonstrated to have acceptable electrocatalysis for EOR especially in alkaline media, when compared to the widely used catalyst of Pt. Therefore, developing novel method for preparing Pd or Pd-based nanoparticle catalysts has been attractive particularly in the field of electrochemical research. Summarily, two typical methods, i.e., chemical reduction method [5] and electrochemical method [6], for fabricating Pd nanoparticles have been developed. In the chemical reduction method [5], the reducing agent could deliver its electrons to the palladium ions, as a result, Pd nanoparticles were prepared. While, in the electrochemical method [6], palladium ions could accept the electrons released from the external power (via the electrochemical apparatus), leading to the formation of Pd nanoparticles. It has been reported that the crystallinity and morphology as well as the electrocatalytic activity of the obtained Pd nanoparticles were closely related to the electrochemical conditions applied. Our previous work [7] has demonstrated that palladium oxide (PdO) had a certain electrocatalytic activity towards EOR. Thus, one idea came into being. Can we electroplate metallic Pd particles onto the surface of PdO to form a novel kind of electrocatalyst for EOR? To the best of our knowledge, the preparation of metallic Pd nanoparticles onto the system that contained PdO and graphene using a cyclic voltammetry (CV) method has not been reported so far.

In this work, a proper amount of PdO and graphene were firstly mixed in distilled water to generate a suspension solution. And then the suspension solution was pyrolyzed under a certain condition. Subsequently, the well washed and dried products were coated on the surface of a glassy carbon (GC) electrode. Lastly, the obtained electrode was potentially swept in a potential range to harvest the CV-treated PdO/G GC electrode. Interestingly, it was found that the CV-treated PdO/G GC electrodes prepared with various scanning rates showed rather different electrocatalytic activities for EOR. The results obtained from electrochemical measurements effectively indicated that CV-treated PdO/G composite material could be employed as electrocatalysts towards EOR, which is very beneficial to the development of electrocatalyst for EOR.

2. EXPERIMENTAL

2.1 Materials

Graphene was provided by the Fengfan Co., Ltd. **(**China). All the electrodes were purchased from Tianjin Aida Co., Ltd (China). All the chemicals were of analytical grade and used as-received. Doubly distilled water was utilized to produce the aqueous solutions.

2.2 Preparation of pyrolysis-treated PdO/G samples

Firstly, 4.0 mg PdO and 10.0 mg graphene were dispersed in 4mL doubly distilled water, generating a suspension solution. And then, the suspension solution was ultrasonicated for 30 min. Secondly, the suspension solution was placed in an autoclave, and then the well sealed autoclave was put in a muffle furnace. It should be noted that the temperature of the muffle furnace was maintained at 200 ºC for 2 hours to finish the pyrolysis treatment. Lastly, the temperature of the muffle furnace was naturally cooled down to the room temperature, subsequently, the produced samples were filtered and washed several times by distilled water and dried in ambient condition, giving rise to the formation of pyrolysis-treated PdO/graphene catalysts.

2.3 Preparation of CV-treated PdO/G modified GC electrode

Prior to the preparation of the CV-treated PdO/G coated GC electrode, pyrolysis-treated PdO/G-coated GC electrodes were fabricated first. In brief, the section of a GC electrode (diameter was 3 mm) was carefully burnished using alumina powder suspensions, and then the well-polished GC electrode was washed with copious distilled water for several times to produce a clean substrate. The pyrolysis-treated PdO/G modified GC electrode was produced by dropping catalyst ink onto the well polished GC electrodes. It should be mentioned that the catalyst ink was fabricated by dispersing 1 mg of above pyrolysis-treated PdO/G catalysts into 1 mL Nafion ethanol solution (The Nafion content was 0.1 wt.%). After 20 min ultrasonication, 15 μL of catalyst ink was dropped onto the well polished GC electrodes. After drying in air, the pyrolysis-treated PdO/G-coated GC electrodes were created.

A traditional three-electrode cell was used to prepare the CV-treated PdO/G coated GC electrode. Namely, in this system, a pyrolysis-treated PdO/G-coated GC electrode, a saturated calomel electrode (SCE) and a platinum wire were employed as the working electrode, reference electrode and counter electrode, respectively. And then the working electrode was potentiostatically cycled between 0 and -0.9V for 50 cycles in an electrolyte solution containing 0.5M Na_2SO_4 and 10^{-3} M $PdCl_2$ at various scan rates. To distinguish the prepared electrodes, the electrodes potentially cycled at the scan rate of 5, 10, 50, 90 mV s^{-1}, were denoted as catalyst **a**, **b**, **c** and **d**, respectively.

2.4 Characterizations

The morphologies of samples were examined by scanning electron microscopy (SEM, HITACHI, S-570) and transmission electron microscopy (TEM, HITACHI, H-7650). Energy Dispersive X-Ray Spectroscopy (EDS) spectrum analysis was carried out on a X-ray energy instrument (EDAX, PV-9900, USA). Electrochemical measurements were carried out on a CHI 660B electrochemical working station (Shanghai Chenhua Apparatus, China) connected to a personal computer.

In the electrocatalytic measurements, a solution of 1 M KOH containing 1 M C_2H_5OH was employed to examine the electrocatalytic activity of the prepared catalysts towards EOR. - prepared CV-treated PdO/G modified GC electrode, a platinum wire and a saturated calomel electrode (SCE) were, respectively, utilized as the working electrode, counter electrode and reference electrode. All potentials in this work were reported with respect to the SCE electrode. All the experiments were performed at room temperature.

3. RESULTS AND DISCUSSION

3.1 Morphology characterization

The morphologies of the prepared samples observed by SEM are given in Fig. 1. Apparently, in all images, the irregular sheets of graphene are observed clearly, indicating that the main morphology of graphene was not destroyed by the pyrolysis and CV treatment. Also, close inspection revealed that some smaller particles were immobilized on the surface of graphene. According to the previous report [8], the electrocatalytic activity of the prepared samples should be ascribed to the presence of small particles since graphene itself has no electrocatalytic ability towards EOR. It seemed that more amounts and much smaller particles were present in image b **(**as shown by the red-circled part) in comparison with other images. To the best of our knowledge, this is the first time to report the morphology of the CV-treated composite particles that contained PdO and graphene.

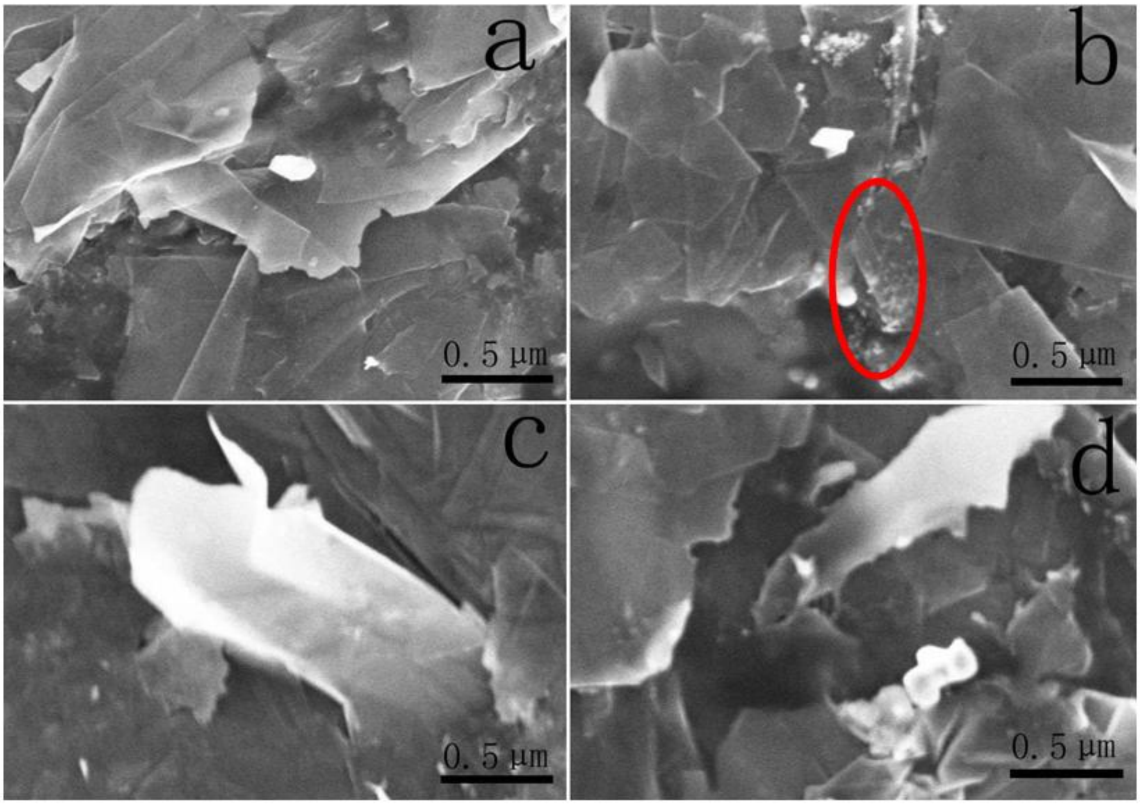

Figure 1. SEM images for all prepared CV-treated PdO/G catalysts. Image **a**, **b**, **c** and **d** represented catalyst **a**, **b**, **c** and **d**.

The TEM images for these four kinds of catalysts are illustrated in Fig. 2. Evidently, the surface of graphene were coated by many small particles, though the agglomeration of particles was seen in image c. Globular particles with an average size of ~35 nm were observed for catalyst **a**, and irregular particles with an average size lower than 10 nm were exhibited by catalyst **b**. Although the particle size of catalyst **c** (about 25 nm) was smaller than that of sample **a**, severe agglomeration of particles occurred. The particles of agglomeration **d** had a particle size of about 20 nm, and it appeared that catalyst **d** had a more uniform particle size distribution relative to other catalysts. Therefore, catalyst **b** showed the smallest particle size among all the catalysts. Generally, when the loadings of catalysts were same, the contacting area between the catalyst and the electrolyte would become larger when the particle size of the catalysts got smaller. That is to say, catalyst **b** should have the largest contacting area when compared to other catalysts if the loadings were identical. According to the Tafel equation [9], the over-potential would be greatly decreased due to the declined current density, which was very advantageous to an electrochemical reaction. Hence, catalyst **b** may exhibit better electrocatalytic activity relative to other catalysts.

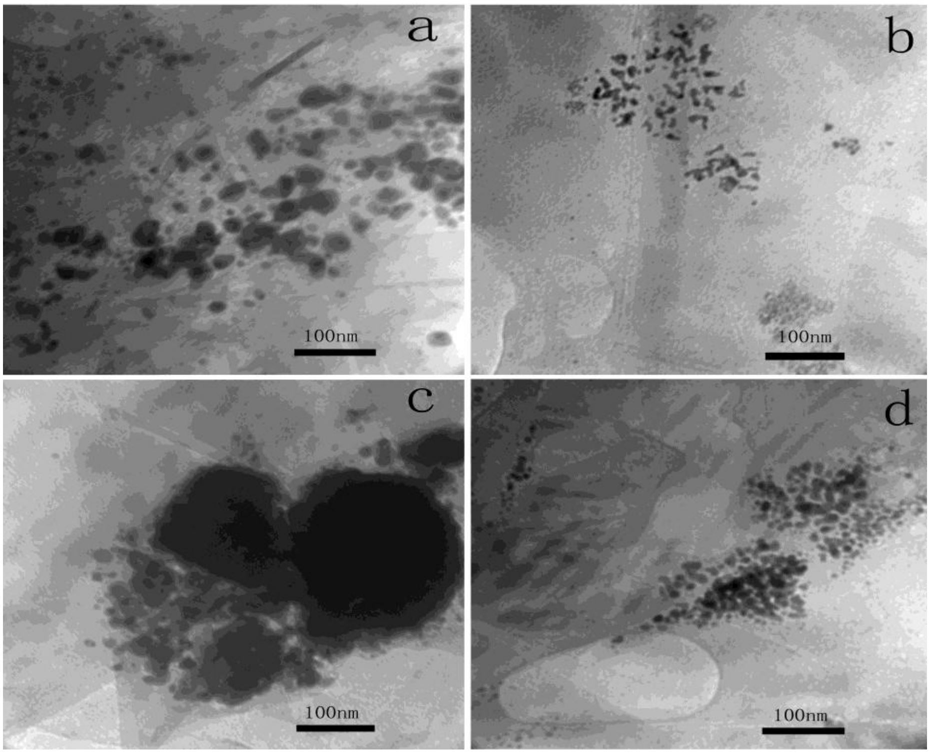

Figure 2. TEM images for all the prepared CV-treated PdO/G catalysts. Image **a**, **b**, **c** and **d** stood for sample **a**, **b**, **c** and **d**.

To further analyze the chemical composition of the as-prepared samples, EDS analysis was also performed (figure not displayed). Besides the presence of elements C and O, the atomic contents of Pd for catalysts **a**, **b**, **c** and **d** were detected to be 13.1%, 27.2%, 5.7% and 7.7%, respectively. Obviously, for all catalysts, the atomic content of Pd should be close to each other if a reversible electrochemical reaction occurred during the CV treatment. Thus, it can be inferred that the electrochemical reaction occurring in the CV treatment was irreversible. Thus, it was concluded that the potential scanning rate was an important factor which could also affect the composition of the resultant catalysts.

3.2. Electrocatalytic performance

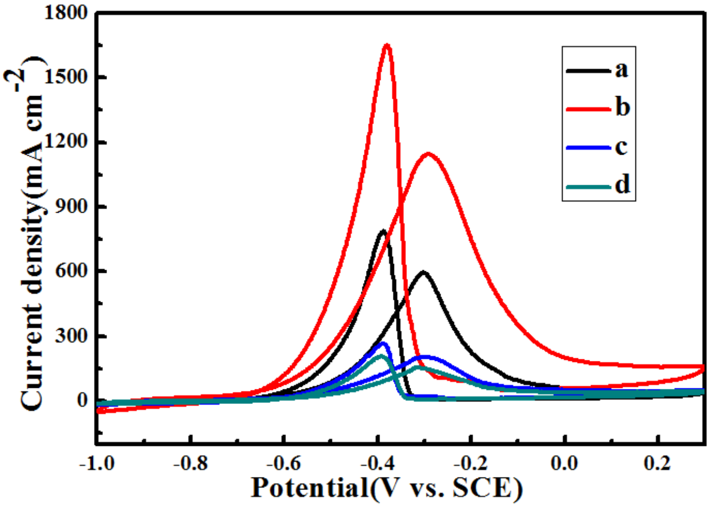

Figure 3. Cyclic voltammograms (CVs) obtained on the CV-treated PdO/G catalysts-coated GC electrodes in 1M KOH having 1M C_2H_5OH solution at the scan rate of 50 mV s^{-1}. The black, red, blue and green curves were measured on the catalyst **a**, **b**, **c** and **d**-coated GC electrode.

The cyclic voltammograms (CVs) of EOR on all the prepared catalysts were measured at the scan rate of 50 mV s^{-1} in a solution of 1 M KOH containing 1M C_2H_5OH and displayed in Fig. 3. Obviously, in all CV curves, one oxidation peak centered at ~-0.30V in the positive direction potential sweep and one centered at ~-0.38 V in the negative direction potential sweep were exhibited clearly. This result effectively indicated that all the prepared CV-treated PdO/G catalysts had electrocatalytic ability for EOR. It should be noticed that the shapes of above CV curves resembled those measured on the Pd-coated GC electrode [10]. According to the prior works concerning EOR [10], the peak current and onset potential are two key parameters which could directly reflect the elctrocatalytic activity of a catalyst for EOR. For the oxidation peaks appearing in the positive direction potential sweep, the peak currents and onset potentials for catalyst **a**, **b,** **c** and **d**, were roughly estimated to be 591 mA cm^{-2} and -0.58V, 1141 mA cm^{-2} and -0.65V, 205 mA cm^{-2} and -0.50V, 154 mA cm^{-2} and -0.49V, respectively. Thus, catalyst **b** showed the largest peak current and most negative onset potential when compared to other catalysts, suggesting that catalyst **b** had the best electrocatlytic activity towards EOR among all the prepared catalysts. Also, this result strongly proved that the potential scanning rate was an important factor in determining the electrocatalytic activity of a catalyst. Probably, potential scanning rate could be utilized as a powerful tool to adjust the electrocatalytic activity of a catalyst. Evidently, when the particle size of a catalyst became smaller, the contacting area between the electroactive substance (in electrolyte) and the catalyst would be greatly increased. Meanwhile, the amount of active sites would be significantly enhanced as the content of Pd was augmented. Thus, it was reasonable to think that the smaller particle size and higher content of Pd of catalyst **b** should be responsible for its superior electrocatalytic activity.

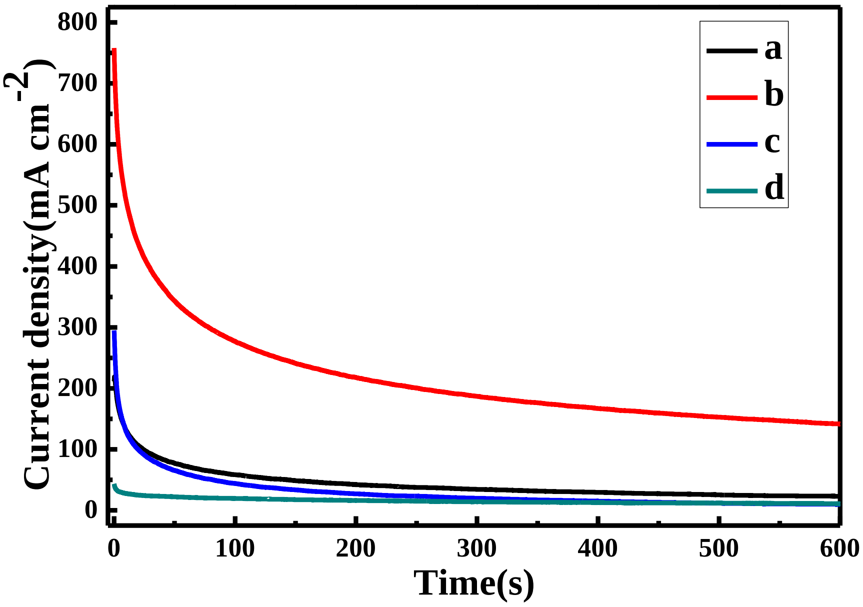

Figure 4. Chronoamperometry curves of various CV-treated PdO/G catalysts modified GC electrodes recorded in 1M KOH +1M C_2H_5OH at -0.24 V. The black, red, blue and green curves were measured on the catalyst **a**, **b**, **c** and **d**-coated GC electrodes.

The technique of chronoamperometry has been extensively employed as a powerful tool to evaluate the durability of an electrocatalyst [11]. The chronoamperometric (CA) curves of the various catalysts-modified GC electrodes in 1 M KOH + 1M C_2H_5OH solution were recorded at -0.24 V as presented in Fig. 4. In the initial stage, a sharp decrease in current density was observed for all the curves. Commonly, the sharp drop of current density was originated from the electric double layer of an electrode, which was closely related to the intermediates adsorbed on the surface of the electrode. Thus, it indicated that catalyst **b** had more resistance to poisoning when compared to other catalysts. Besides the sharp drop of current density in the initial stage, a relatively stable current was exhibited in the left testing period. As addressed in the previous work [11], the stable current in the CA curve was called as polarized current which was mainly ascribed to the direction electro-oxidation of both ethanol and the intermediates. Apparently, the catalyst **b** delivered the highest current density in the whole testing duration. For example, the current densities on the catalyst **a**, **b**, **c** and **d** were approximately evaluated to be 22.6, 138.3 and 9.1 and 9.0 mA cm^{-2} at 600 s, respectively. This result substantially certified that the catalyst **b** exhibited not only the largest polarized current density but also the best durability and stability among all the synthesized catalysts. Also, this result further illustrated that potential scanning rate was a key factor which could affect the electrocatalytic activity of a composite material that contained PdO and graphene.

3.3. Analysis of the electrocatalytic mechanism

Why did the catalyst **b**, that was prepared by potential sweep for 50 cycles at the scan rate of 10 mV s^{-1}, exhibit the best electrocatalytic activity for EOR among all the catalysts? To discuss the possible reasons, the last CV curves (the fiftieth potential cycling) of all the pyrolysis-treated PdO/G coated GC electrodes measured in 0.5M Na_2SO_4 containing 10^{-3} M $PdCl_2$ were also given in Fig. 5. Evidently, for catalyst **a** and **b**, a pair of redox peaks were displayed. While, for catalyst **c** and **d**, no obvious redox peaks were found. According to our previous work [12], for the system having PdO and graphene, some metallic Pd particles could be prepared in the pyrolysis process, thus, a system that contained metallic Pd, PdO and graphene was produced after the pyrolysis treatment. Therefore, the electro-oxidation peaks appearing in Fig. 5 should correspond to the oxidation of metallic Pd, namely, $Pd\text{-}2e \rightarrow Pd^{2+}$. And in the presence of oxygen, PdO was prepared. Correspondingly, for the electro-reduction peak, PdO was electrochemically reduced to be metallic Pd, i.e., $PdO + 2e + H_2O \rightarrow Pd + 2OH^-$. Additionally, the shape of oxidation peak was rather different from that of the corresponding reduction peak. This result effectively suggested that the mechanism of oxidation process differed from that of the reduction process, though the exact mechanism could not be revealed by CV curve only. Commonly, the peak area of the CV curves corresponded to the quantity of electric charge consumed. And a peak with larger area meant that more substances were prepared based on the Faraday Law [13]. Close observation revealed that the reduction peak area was slightly larger than that of the corresponding oxidation peak. That is to say, for catalyst **a** and **b**, more metallic Pd was produced during the potential sweep treatment. Compared to catalyst **a**, more metallic Pd was prepared due to the larger reduction peak area of catalyst **b**. This result was consistent with that of EDS analysis.

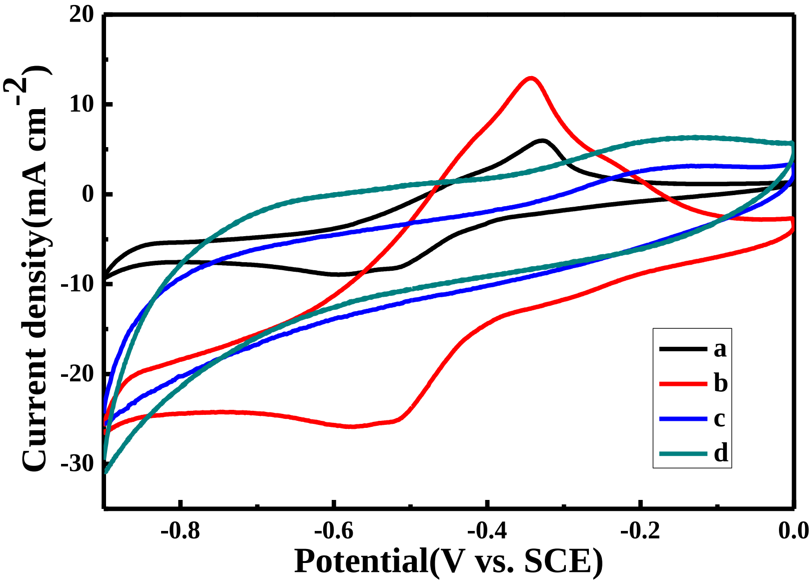

Figure 5. The CV curves obtained in 0.5M Na_2SO_4 solution containing 10^{-3} M $PdCl_2$ for all prepared CV-treated PdO/G coated GC electrodes. The black, red, blue and green curves were recorded at the scan rate of 5, 10, 50, 90 mV s^{-1}.

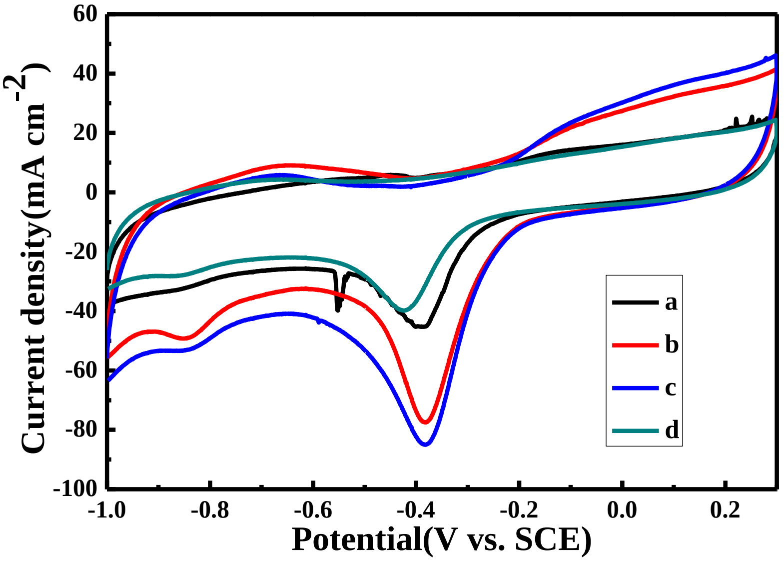

Figure 6. Cyclic voltammograms (CVs) obtained on all prepared CV-treated PdO/G coated GC electrodes in 1M KOH solution at the scan rate of 50 mV s^{-1}. The black, red, blue and green curves were measured on the catalyst **a**, **b**, **c** and **d**-coated GC electrodes.

The CV curves of the prepared catalysts in 1M KOH were also plotted as shown in Fig.6. The large reduction peak centered at about -0.38V should be attributed to the reduction of PdO based on the former works [14]. Therefore, it seemed that catalyst **b** and **c** had more amounts of metallic Pd compared to catalyst **a** and **d**. The weak peaks positioned at about -0.84V should be originated from desorption of hydrogen, namely, $H^+ + e \rightarrow H$. The enhanced currents at about -1.0V were all from the hydrogen evolution. Thus, it appeared that more hydrogen atoms were formed before the hydrogen evolution in catalyst **b** due to its more larger hydrogen desorption peak, compared to other catalysts. The widely accepted electro-oxidation mechanism of ethanol has been proposed as follows [14].

$$CH_3CH_2OH \leftrightarrow (CH_3CH_2OH)_{ads} \quad (1)$$

$$(CH_3CH_2OH)_{ads} + 3OH^- \rightarrow CH_3CO_{ads} + 3H_2O + 3e^- \quad (2)$$

$$OH^- \leftrightarrow OH_{ads} + e^- \quad (3)$$

$$CH_3CO_{ads} + OH_{ads} \rightarrow CH_3COOH \quad (4)$$

$$CH_3COOH + OH^- \rightarrow CH_3COO^- + H_2O \quad (5)$$

Thus, according to above steps, more created OH^- can yield a larger amount of OH_{ads}, which can greatly accelerate the step (2), (3), (4) and (5). As analyzed above, more OH^- ions were formed at the surface of catalyst **b**, which would be favorable to the oxidation of ethanol.

To acquire more information of the resultant catalysts, electrochemical impedance spectroscopy (EIS) analysis was also conducted. Bode plots, one typical kind of curve in EIS, for all prepared catalysts are given in Fig. 7. It can be observed that all the electrodes showed a symmetric peak in the relatively lower frequency region, and as addressed previously, the symmetric peak[15] generally stemmed from the relaxation process of the electrode | solution interface. The phase angles at 1Hz for the catalyst **a**, **b**, **c** and **d** electrodes were evaluated to be approximately 59°, 61°, 71° and 40°, respectively. Theoretically, an ideal capacitive system should give a phase angle of *ca.* −90° [15] in the Bode plot at the lowest frequency point. Hence, it could be deduced that all these four electrodes really acted as quasi-capacitors. Also, careful observation could reveal that the peak frequencies of the symmetric peak in the lower frequency region for the electrode **a**, **b**, **c** and **d** were about 10Hz, 100Hz, 125 Hz and 316 Hz, respectively. That is to say, the relaxation process of the electrode | solution interface for catalyst **b** occurred in the lower frequency region. Or in other words, the interactions between the electrode and electrolyte were notable in catalyst **b** when compared to other catalysts. Above results documented that the surface structures of these four electrodes were different from each other, and the surface structure of catalyst **b** was favorable to the electro-oxidation of ethanol.

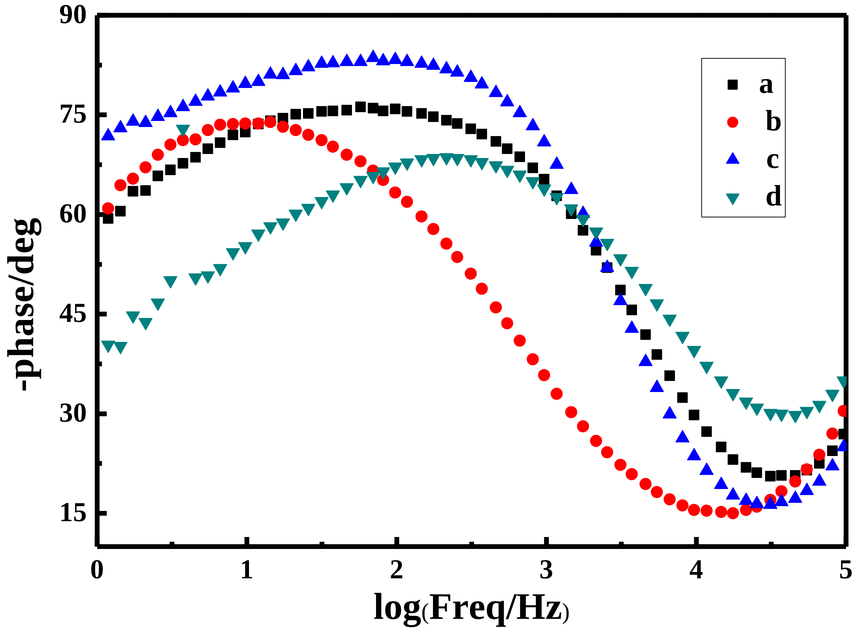

Figure 7. Bode plots for the various PdO/G coated GC electrodes obtained in 1 M KOH +1 M C_2H_5OH aqueous solution.

4. CONCLUSION

For the first time, the effect of potential scanning rate on the electrochemical performance of the pyrolysis-treated PdO/graphene composite catalyst was examined in this work. The morphologies of the obtained samples were thoroughly characterized by SEM and TEM, the results indicated that the smallest nanoparticles were exhibited as the potential scanning rate was 10 mV s^{-1}(catalyst **b**). The electrocatalytic activities of the resultant PdO/G catalysts for EOR were mainly studied by CV and CA, and the results effectively proved that the potential scanning rate was a key factor which could greatly influence the electrocatalytic activity of the resultant catalysts. Also the 10 mV s^{-1}-treated catalyst delivered the best electrocatalytic activity for EOR among all the prepared catalysts. Presenting a novel method for preparing a novel catalyst that contained PdO and graphene was the major contribution of this work, which was very helpful to the development of electrocatalysts of EOR.

ACKNOWLEDGEMENTS

This work was financially supported by the National Natural Science Foundation of China (No. 21173066), Natural Science Foundation of Hebei Province of China (No.B2015205150 and No.B2011205014).

References

1. W. Du, G. Yang, E. Wong, N. Aaron Deskins, A. I. Frenkel, D. Su and X. Teng, *J. Am. Chem. Soc.*, 136 (2014) 10862.
2. D. R.M. Godoi, H. M. Villullas, F.-C. Zhu, Y.-X. Jiang, S.-G. Sun, J. Guo, L. Sun and R. Chen, *J. Power Sources*, 311 (2016) 81.
3. M. S. Ahmed, D. Park and S. Jeon, *J. Power Sources*, 308 (2016) 180.
4. T. Jurzinsky, P. Kammerer, C. Cremers, K. Pinkwart and J. Tübke, *J. Power Sources*, 303 (2016) 182.
5. H. Erikson, M. Lüsi, A. Sarapuu, K. Tammeveski, J. Solla-Gullón and J. M. Feliu, *Electrochim. Acta*, 188 (2016) 301.
6. S. K. Konda and A. Chen. *Electrochem. Commun.*, 60 (2015) 148.
7. K. Ding, Y. Wang, H. Yang, C. Zheng, Y. Cao, H. Wei, Y. Wang and Z. Guo, *Electrochim. Acta*, 100 (2013) 147.
8. K. Ding, Y. Li, Y. Zhao, L. Liu, H. Gu, L. Liu, S. Qiu, C. He, J. Liu, Q. Wang, Z. Guo, *Electrochim. Acta* , 149 (2014) 186.
9. S.C. Zignani, V. Baglio, D. Sebastián, S. Siracusano and A.S. Aricò, *Electrochim. Acta*, 191 (2016) 183.
10. Y.-H. Qin, Y. Zhuang, R.-L. Lv, T.-L. Wang., W.-G. Wang and C.-W. Wang, *Electrochim. Acta*, 154 (2015) 77.
11. K. Ding, Y. Zhao, Y. Li, J. Zhao, Y. Chen, Y. Wang and Z. Guo, *Int. J. Electrochem. Sci.*, 10 (2015) 969.
12. K. Ding, Y. Zhao, L. Liu, Y. Li, L. Liu, Y. Wang, H. Gu, H. Wei and Z. Guo, *Electrochim. Acta*, 176 (2015) 1256.
13. C. Vautrin-Ul, A. Taleb, J. Stafiej, A. Chaussé and J.P. Badiali, *Electrochim. Acta*, 176 (2015) 1256.
14. Z. X. Liang, T. S. Zhao, J. B. Xu and L. D. Zhu, *Electrochim. Acta*, 54 (2009) 2203.
15. C. Hu, S. Yuan and S. Hu, *Electrochim. Acta*, 51 (2006) 3013.